Molecular Shape of Regular Star Polymers by Monte Carlo Simulations

Alessandra Forni,[†,§] Fabio Ganazzoli,[*,†] and Michele Vacatello[‡]

Dipartimento di Chimica, Politecnico di Milano, via L. Mancinelli 7, I-20131 Milano, Italy, and Dipartimento di Chimica, Università di Napoli, via Mezzocannone 4, I-80134 Napoli, Italy

Received January 22, 1997; Revised Manuscript Received May 5, 1997[⊗]

ABSTRACT: Off-lattice Monte Carlo simulations were performed on linear and 12-arm star polymers in a good-solvent and in the Θ state to investigate both the molecular shape and the size distribution. We find that in a good solvent the star polymer is more spherical than a random walk, the more so the smaller its size is; moreover, a star of finite chain length in the Θ state has a shape more similar to that in good solvent than to that in a random walk because of the excluded-volume restrictions that are particularly relevant in the core region. Both results are at variance with what is found in linear chains. Furthermore, the size distribution of the star is much narrower in a good solvent than in a random walk, approaching somewhat a δ function. This effect is also seen in the strong deformation of the density profile away from the center of mass.

Introduction

The conformational and dynamical properties of star polymers are the object of an increasing interest both from a theoretical viewpoint and because of their technological applications.[1] An interesting aspect of their equilibrium conformation is their large local expansion in the core region, even with respect to linear chains.[2−4] This topic was investigated in detail in our previous off-lattice Monte Carlo studies of 12-arm stars in a good solvent in ref 2, hereafter referred to as paper I. This local expansion is related to a substantial stretching of each arm in the branch-point region and to a strong loss of correlation among bond vectors *across* the branch point (see Figure 5 of paper I). In particular, we found that if the bonds close to the branch point belong to the same arm, their scalar products are essentially constant and are much larger than those far from the branch point; conversely, if they belong to different arms, their scalar products drop by more than 1 order of magnitude. This peculiar conformation allows the best accommodation of the intra- and interarm repulsions and minimizes the entropy loss due to the arm expansion. The same trend had been theoretically predicted in the framework of the configurational normal-mode approach with self-consistent free-energy minimization.[5,6]

In paper I we were mostly interested in the local properties of the star in a good solvent, and the asymptotic properties for $N \rightarrow \infty$ were used only as a check of the simulation procedure. In the present paper, we report some results on the overall molecular shape of a 12-arm star and its size distribution obtained within the same off-lattice Monte Carlo simulations in a good solvent and in the Θ state. The linear chain behavior will also be reported for a comparison. A number of such results have already appeared in the literature,[4,7−9] but all were derived through lattice simulations, to the best of our knowledge. The simulated properties characterizing the molecular shape turned out to be asymptotically independent of the chosen lattice, but this was not so for finite chains: indeed, the actual chain-length dependence of most of these properties could be sharply different for different lattices. Therefore, we shall focus on such aspects in the discussion of our off-lattice simulations both for the good solvent and for the Θ state. After a brief description of our method and of the computed properties, we will report our results. They will be distinguished in descriptors of the chain shape (asphericity and principal axes of the radius-of-gyration tensor) and descriptors of the size distribution (higher even moments of the radius of gyration and of the distance among the free ends and density profiles around the center of mass). The descriptors of chain shape have already been investigated in lattice simulations by other authors,[4,7−9] unlike most descriptors of the size distribution, and shall be compared with our off-lattice simulations.

Chart 1

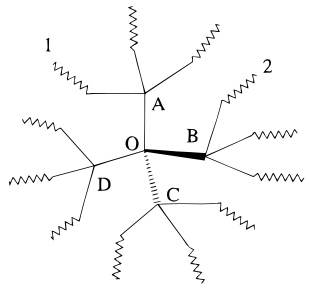

Model and Simulation Method

The polymers are modeled as chains of beads connected by bonds of unit length and interacting through a 6−12 Lennard−Jones potential. We consider star polymers with $f = 12$ arms having the structure shown in Chart 1: four bonds depart from the central branch point O with a fixed tetrahedral geometry, and each bond is followed by three arms that depart from the secondary branch points (A−D) with no further geometrical constraint. We generated stars with total number of bonds, $N = mf - 8$, up to 472, m being the arm length. Linear chains were also considered, for comparison, as a special case of a star with $f = 2$, and $N = mf$. In this case, we chose two "arms" passing through the central "branch" point O (e.g., arms 1 and 2 in Chart 1).

We performed off-lattice Monte Carlo simulations using a slightly modified version of the PIVOT algorithm,[10] following

† Politecnico di Milano.
‡ Università di Napoli.
§ Present address: Dipartimento di Chimica Fisica ed Elettrochimica, Università di Milano, via Golgi 19, I-20133 Milano, Italy.
⊗ Abstract published in *Advance ACS Abstracts,* July 1, 1997.

S0024-9297(97)00067-3 CCC: $14.00

the strategy outlined in detail in paper I. A Monte Carlo transition is realized by first randomly selecting one bead; then the smaller of the two polymer portions connected to it is rigidly rotated at random around a random axis through the selected bead. The new configuration is accepted or rejected according to the Metropolis algorithm.[11]

In order to describe the good-solvent regime, we used the same energy parameter of the Lennard−Jones potential as in paper I, i.e. $\epsilon/k_BT = 0.05$. For the Θ state, we used an energy parameter that yields a linear dependence on N of the mean-square radius of gyration $\langle S^2\rangle$ and of the mean-square end-to-end distance $\langle R^2\rangle$ (in this case *all* the end-to-end distances in the star were averaged), so that $\langle S^2\rangle \propto N^{2\nu_S}$ and $\langle R^2\rangle \propto N^{2\nu_R}$, with $2\nu_S = 2\nu_R = 1$. This procedure differs from the experimental definition of the Θ state, which requires a vanishing second virial coefficient, but can still be used to reproduce satisfactorily the Θ state, which is found within a small temperature range proportional to $N^{-1/2}$. The energy parameter commonly accepted for lattice Monte Carlo simulations of the Θ state on a simple cubic lattice[7,8,12] or off-lattice,[13] $\epsilon/k_BT = 0.275$, turns out to be also a suitable value for our off-lattice simulations. However, we encountered great difficulties in simulating long chains in this regime with our algorithm because of an incomplete relaxation of the central portions of the longest chains, even after a huge number of Monte Carlo steps.[13,14] Of course, this is due to the more compact conformation of the Θ state, which makes the relaxation of long chains exceedingly lengthy because of the self-avoiding condition. With the above-mentioned energy parameter, in the case of stars, we obtained the exponent $2\nu_S = 1.003$ for $\langle S^2\rangle$ and a slightly larger value for $\langle R^2\rangle$, $2\nu_R = 1.033$, in the range $112 \le N \le 304$, corresponding to arm lengths $10 \le m \le 26$. On the other hand, the exponents of the linear chains are $2\nu_S = 1.066$ and $2\nu_R = 1.059$ with $N \le 80$ and "arm" lengths $m \le 40$. Apart from the exponent $2\nu_S$ of the star, these "apparent" exponents are still changing with N, being significantly smaller if the shorter chains are ignored. Therefore, scaling corrections accounting for the finite size of the chains are necessary (see also paper I and ref 4): if $\langle S^2\rangle/N$ and $\langle R^2\rangle/N$ as plotted vs $N^{-1/2}$, the data follow a straight line with a negative slope in all cases, indicating that the chains are indeed in the Θ state and that such corrections are not yet negligible (only in the star does $\langle S^2\rangle/N$ yield a constant value).

Due to these chain-length limitations, extrapolation of the results to $N \to \infty$ in the Θ state must be considered with some caution; therefore, for each property we first discuss the good-solvent behavior, and afterward we comment about the most relevant differences in the Θ state. Nonetheless, it must be noted that our asymptotic values do not show any significant difference from the available literature results (see later).

Chain-length dependence of the Monte Carlo results was determined in different ways according to the regime considered. A satisfactory linear dependence, useful for extrapolation to $N \to \infty$, was obtained by plotting the results against $N^{-1/2}$; however, some data obtained for the stars in the Θ state could be fitted only by a second order polynomial (see also ref 8). We report also results for the random walk, for a comparison with the analytical values, whenever these are available. In this case, a linear dependence was obtained by plotting the results against N^{-1}.

The estimated errors on the points shown in the figures are smaller than the symbol sizes and those on the asymptotic values reported in the text and in the tables are within ±1 on the last digit for the good-solvent state and the random walk and within ±2 for the Θ state.

Computed Properties. A first set of conformational properties examined in this paper is related to the shape of the polymer molecules. It is well-known[4,9,15−18] that the average conformation of an isolated macromolecule of any architecture with respect to its principal axes is not spherical. The asymmetry of the molecule can be characterized through the tensor of inertia **T**:[16,17]

$$T_{ij} = \frac{1}{N+1}\sum_{l=1}^{N+1}(X_{il} - X_{i,\mathrm{com}})(X_{jl} - X_{j,\mathrm{com}}) \qquad (1)$$

Table 1. Reduced Moments of S^2 for Linear Chains and Stars, Extrapolated to $N \to \infty$.

		$\langle S^{2n}\rangle/\langle S^2\rangle^n - 1$			
	n	analytical[a]	random walk	good solvent	Θ solvent
linear	2	$^4/_{15} = 0.2667$	0.268	0.190	0.253
	3	$^{316}/_{315} = 1.0032$	1.005	0.671	0.931
	4	$^{904}/_{315} = 2.8698$	2.860	1.725	2.535
star	2	0.0383	0.038	0.013	0.029
	3	0.1185	0.117	0.040	0.089
	4		0.245	0.081	0.183

[a] From ref 21 and the expressions[18]

$$\sigma_2^S = \frac{4(15 - 14/f)}{15f(3 - 2/f)^2}$$

$$\sigma_3^S = \frac{4(2835 - 3528/f + 772/f^2)}{315f(3 - 2/f)^3}$$

X_{il} is the i-th cartesian component of the position vector of the lth bead, and $X_{i,\mathrm{com}}$ is the corresponding component of the center-of-mass vector. Indicating with Tr the trace of **T** and with λ_i its eigenvalues, the chain shape can be described by the "asphericity"[19]

$$A = \frac{\langle Tr^2 - 3M\rangle}{\langle Tr^2\rangle} \qquad (2)$$

with $M = \lambda_1\lambda_2 + \lambda_2\lambda_3 + \lambda_3\lambda_1$. This parameter ranges from zero for spherically symmetric chains to one for rod-shaped chains. For random-walk linear and star polymers its analytical expression is known in the infinite-chain limit:[20]

$$A = \frac{10(15 - 14/f)}{15f(3 - 2/f)^2 + 4(15 - 14/f)} \qquad (3)$$

A more specific characterization of the chain shape is given by the eigenvalues of **T**, λ_i, referred to as the principal components of the radius-of-gyration tensor, i.e. the components of S^2 along the principal axes of inertia of the chain.[16,17] The ratios of their average values, $\langle\lambda_1\rangle:\langle\lambda_2\rangle:\langle\lambda_3\rangle$, where we shall adopt the convention $\lambda_3 > \lambda_2 > \lambda_1$, indicate the departure of the chain from the spherical symmetry along three orthogonal directions. Alternatively, the chain shape can be characterized by the average eigenvalues, usefully normalized by the mean-square radius of gyration; these were also denoted[9] as "shape factors" $sf_i = \langle\lambda_i\rangle/\langle S^2\rangle$ ($i = 1, 2, 3$). Unlike the asphericity, the analytical expression of the λ_i's is not available even for random walks.

Next, we analyze the size distribution of the polymers through the average n-moments of S^2 and R^2, $\langle S^{2n}\rangle$ and $\langle R^{2n}\rangle$ ($n = 2, 3, 4$). These moments will be reported as $\sigma_n^S = (\langle S^{2n}\rangle - \langle S^2\rangle^n)/\langle S^2\rangle^n$ and $\sigma_n^R = (\langle R^{2n}\rangle - \langle R^2\rangle^n)/\langle R^2\rangle^n$. The random-walk analytical values of σ_n^R for linear chains are known, being the reduced moments of a Gaussian distribution, as well as σ_n^S, $n = 2$ and 3, for either architecture,[18,21] and are reported in Tables 1 and 2, together with our results. A related piece of information is provided by the density profile of the beads around the center-of-mass of the polymer, $\rho(\mathbf{r})$. We computed the radial density profile $4\pi r^2\rho(r)$ by considering concentric shells of unitary thickness centered on the chain center of mass and finding the number of beads located in each shell. The quantities were then normalized through the shell volume.

Results and Discussion

I. Chain Shape. The asphericity, A, of the stars and of the linear chains obtained with the present simulations is shown in Figure 1. (Here, as well as in the following figures, the upper N^{-1} scale is arbitrarily expanded in order to show more clearly the N-dependence of the random-walk results.) A remarkable dif-

Table 2. Reduced Moments of R^2 for Linear Chains and Stars, Extrapolated to $N \to \infty$

		$\langle R^{2n}\rangle/\langle R^2\rangle^n - 1$			
	n	analytical[a]	random walk	good solvent	Θ solvent
linear	2	$^2/_3 = 0.6667$	0.668	0.521	0.682
	3	$^{26}/_9 = 2.8889$	2.890	2.049	2.905
	4	$^{32}/_3 = 10.6667$	10.619	6.496	10.310
star	2		0.059	0.030	0.057
	3		0.182	0.090	0.175
	4		0.389	0.185	0.370

[a] Higher moments of a Gaussian distribution.

ference between the two polymer structures concerns the asphericity values: the star with 12 arms is a nearly spherical object (i.e., A is close to zero) owing to its structure, unlike the linear chain, which is strongly anisotropic. In fact, the central branch point constrains the star arms to a more uniform distribution. This effect is increasingly important with increasing f, and a spherical object with $A = 0$ is expected when $f \to \infty$. The asymptotic values for the random-walk chains ($A = 0.527$ for the linear chain and $A = 0.0919$ for the 12-arm star) are in a good agreement with the analytical ones obtained with eq 3, $A = 10/19 = 0.5263$ and $A = 0.0922$, respectively.

In a good solvent, the star and the linear polymers depart from the random walk in opposite ways. The linear chain is slightly *less* spherical than the random walk, as shown by the asympotic value $A = 0.547$ of Figure 1, left panel, while finite chains are even less spherical. Very similar asymptotic values were obtained with Monte Carlo simulations on the face-centered cubic lattice[4] (FCC lattice, for short) and on the tetrahedral lattice,[9] i.e., 0.55 and 0.545, respectively. However, these simulations showed an opposite chain-length dependence: on the tetrahedral lattice, finite chains are less spherical than the infinite chain (i.e., they have a larger A), in agreement with our result, whereas on the FCC lattice the opposite behavior is found. This difference might originate from the lattice type,[9] which determines the local properties of the chain or, in other words, its stiffness. Extensive simulations of nonreversal random walks on different lattices by Zifferer and Olaj support this conclusion:[22] for instance, the asphericity tends to the asymptotic value from above in the tetrahedral lattice and from below in the four-choice cubic lattice. In the former case we have stiffer chains, since for instance we can have ring closure after a minimum of six bonds, whereas in the latter case the ring closure may take place after only four bonds. In our off-lattice simulations, the chain stiffness is related to the width of the Lennard−Jones potential we adopted. Thus, local effects strongly influence the behavior of finite linear chains, although being asymptotically irrelevant.

On the other hand, the star in a good solvent is much *more* spherical than the random-walk star, having $A = 0.0633$ for $N \to \infty$. This asymptotic result is very close to the value $A = 0.066$ obtained for 12-arm stars on the tetrahedral lattice.[9] Moreover, from the power law $A \propto f^{-1.19}$ obtained in ref 4 from Monte Carlo simulations of stars with $f = 3-6$ arms on the FCC lattice, one would indeed get $A = 0.066$ for $f = 12$. Unlike the linear chain, the asphericity of the star increases with N. Furthermore, the star shows a stronger N-dependence than the linear chain. A similar trend was also observed in all lattice simulations;[4,9] therefore, it appears that the topological constraint of the star is more important than the local effects related to the chain stiffness.

The departure of the asphericity of star and linear chains in a good solvent from the random-walk values is due to the nonuniform expansion of the polymers.[9] In the largely anisotropic linear chain, the expansion is more pronounced in the directions of the longer ellipsoidal axis of the chain (see also later), causing a further increase of the anisotropy. This result is in keeping with the molecular-mass dependence of the expansion factor $\alpha^2_S = \langle S^2\rangle/\langle S^2\rangle_{RW}$, approximately proportional to $N^{1/5}$, which suggests that a greater expansion is to be expected just in the regions where most beads are concentrated. In star polymers, the nonuniform expansion is concentrated *within* each arm near the branch point, in order to minimize the interarm interactions. As discussed in paper I, a strong loss of correlation among the different arms results from this nonaffine expansion, causing a greater uniformity in the spatial distribution of the arms around the branch point with respect to the random walk and thus a greater sphericity. This effect is more pronounced the shorter the arms are, so that small stars are more spherical than large ones, thus explaining the trend of A observed in Figure 1.

The same considerations also apply to the curves of the principal components of the radius-of-gyration tensor, λ_i, $i = 1, 2, 3$. The asymptotic values of the shape factors for linear random walk ($sf_i = 0.0633, 0.172, 0.765$ for $i = 1-3$), corresponding to the ratios $\langle\lambda_1\rangle:\langle\lambda_2\rangle:\langle\lambda_3\rangle = 1:2.71:12.1$, are in agreement with previous simulation results[8,17,23] and indicate a strong departure from the spherical shape toward a prolate ellipsoid. In a good solvent, the largest shape factor increases somewhat, while the others become slightly smaller ($sf_i = 0.0556, 0.163, 0.774$ for $i = 1-3$), so that their ratios increase to 1:2.92:13.9. These values show that the linear chain undergoes a greater relative expansion along the principal component of greater size, as discussed above, and thus it displays an even larger prolateness. The above values compare well with simulation results of linear chains on the tetrahedral lattice,[9] including also the slight dependence of these quantities on the chain length.

The shape factors of the star are reported in Figure 2. The asymptotic values in a good solvent ($sf_i = 0.203, 0.320, 0.473$ for $i = 1-3$) show a smaller spread than expected for the random walk ($sf_i = 0.184, 0.310, 0.506$ for $i = 1-3$); thus, the corresponding ratios $\langle\lambda_2\rangle/\langle\lambda_1\rangle$ and $\langle\lambda_3\rangle/\langle\lambda_1\rangle$ drop from the random-walk values of 1.69 and 2.75 to the good-solvent values of 1.57 and 2.31, which indicates an even more spherical shape. In the good-solvent case, a pronounced chain-length dependence of the shape factors is found, in particular for sf_1 and sf_3, the former decreasing and the latter increasing with increasing N (see Figure 2). Also in this case, these results are in excellent agreement with the simulation results of 12-arm stars on the tetrahedral lattice.[9]

The two polymer structures differ in their shape also in the Θ state. The asphericity of the linear chain is very similar to the asphericity of the random walk and compares very well with the result obtained by Monte Carlo simulations of linear chains on the tetrahedral lattice,[9] including also the weak dependence on the chain length (incidentally, this result suggests that our use of relatively short chains is quite irrelevant). Interestingly, our asymptotic value, $A = 0.517$, is much smaller than the good-solvent value and slightly but

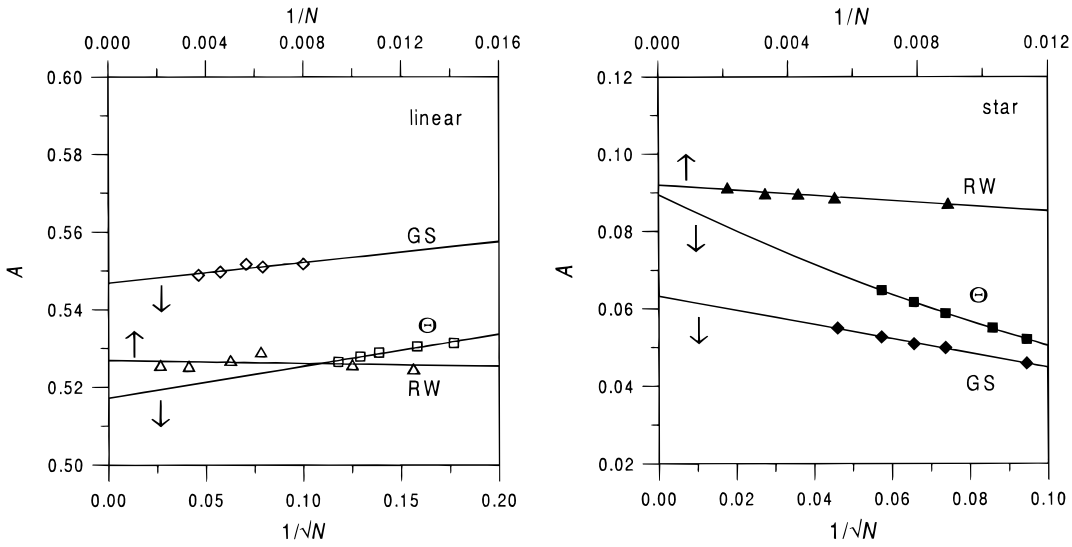

Figure 1. Asphericity, A, of linear and star polymers (left and right panels with empty and filled symbols, respectively) in a good solvent (diamonds with GS label) and in the Θ state (squares with Θ label) plotted as a function of $N^{-1/2}$ (lower abscissa). The results for the random-walk polymers (triangles with RW label) are reported as a function of N^{-1} (upper abscissa). The best-fit curves are also shown.

significantly smaller than the random-walk value. On the other hand, the star asphericity has a marked dependence on N, as shown in Figure 1, right panel: in particular, for finite chain lengths, A is only slightly larger than in a good solvent, indicating that strong interarm repulsions still persist in the Θ state, in particular close to the branch point. However, in longer chains, A increases to an asymptotic value, $A = 0.0894$, that is much larger than the good-solvent value and similar to, though still somewhat smaller than, the random-walk value. This behavior is easily understood by considering that the interarm repulsions in the core region become less important for increasing N, and are irrelevant for $N \rightarrow \infty$. In this limit, only the chain topology matters, and the overall shape of the star in the Θ state becomes nearly indistinguishable from the random-walk shape, analogous to what was observed for the linear chain. This chain-length dependence confirms the simulation results on the tetrahedral lattice,[9] where the stars in the Θ state are asymptotically closer to the corresponding nonreversal random walk than linear chains.

In a Θ solvent, the asymptotic shape factors of the linear chain, $sf_i = 0.0657$, 0.174, 0.741 ($i = 1-3$), are very close to the random-walk values, only sf_1 and sf_3 being marginally different. Thus, the corresponding ratios of the average principal components of the radius of gyration are $\langle\lambda_1\rangle:\langle\lambda_2\rangle:\langle\lambda_3\rangle = 1:2.65:11.3$, i.e., slightly smaller than those for the random walk, unlike what happens in a good solvent. In the star, the asymptotic shape factors, 0.184, 0.312, and 0.508, as well as their ratios, 1:1.70:2.76, are equal to the random-walk values. These results are in good agreement with those obtained by Zifferer for the tetrahedral lattice;[9] it should be added that Bruns and Carl[8] simulated linear and star chains with four, five, and six arms on the simple cubic lattice at the true Θ state, defined by the vanishing of the second virial coefficient, unlike ours and Zifferer's simulations, and found again that the ratios of the principal components are equal to the random-walk values. As to the behavior of the finite star chains, what was said above for the star asphericity still applies: the shape factors of small stars in the Θ state display a pronounced dependence on N and show a crossover from a "good-solvent" behavior for small N to the random-walk behavior at large N, again in agreement with the results obtained on the tetrahedral lattice.[9]

II. Size Distribution. In Tables 1 and 2 we summarize the asymptotic values of the reduced n-moments of S^2 and R^2 ($n = 2$, 3, 4), $\sigma_n^S = (\langle S^{2n}\rangle - \langle S^2\rangle^n)/\langle S^2\rangle^n$ and $\sigma_n^R = (\langle R^{2n}\rangle - \langle R^2\rangle^n)/\langle R^2\rangle^n$. In order to discuss the chain-length dependence of the star, we report in Figure 3 the curves of the reduced moments of S^2 with $n = 2$ and $n = 4$, the curves with $n = 3$ being midway in any case. Note that the deviations of σ_n^S and σ_n^R from 0 indicate the departure of the size distribution from a δ function, characterized by only one possible size value.

The distribution of S^2 is always narrower than the distribution of R^2, because it includes *all* the distances among the beads (indeed S^2 is just their instantaneous average), whereas R^2 is simply one of them. In fact, the distribution function of an *average* quantity is always narrower than that of an *individual* quantity forming that average. As predicted by Šolc,[18] in the star the distribution of both S^2 and R^2 is significantly sharper than in the linear chain, for any solvent condition. In fact, all the reduced moments are expected to decrease with the arm number f, so that σ_n^S and σ_n^R approach zero when $f \rightarrow \infty$.[18] This dependence on f is due to the loss of conformational freedom of the arms, imposed by the branch point, causing a reduction in the fluctuations of the distances among the beads. This effect is more pronounced with increasing f, determining the narrowing of the size distributions.

In the good solvent regime, both linear and star polymers have a narrower size distribution than the random-walk polymer. This narrowing is due to excluded-volume repulsions, which sterically constrain the beads in both structures, lowering the fluctuations of the distances among them. The effect is more pronounced in star than in linear chains, where furthermore the chain-length dependence is quite weak. This is another manifestation of the large constraint imposed by the molecular architecture. Note that the size distribution of the star with $f = 12$ in a good solvent approaches rather closely a δ function.

On the other hand, in the Θ state a different behavior between the two polymer structures is found. In the linear chain, the asymptotic values of the reduced

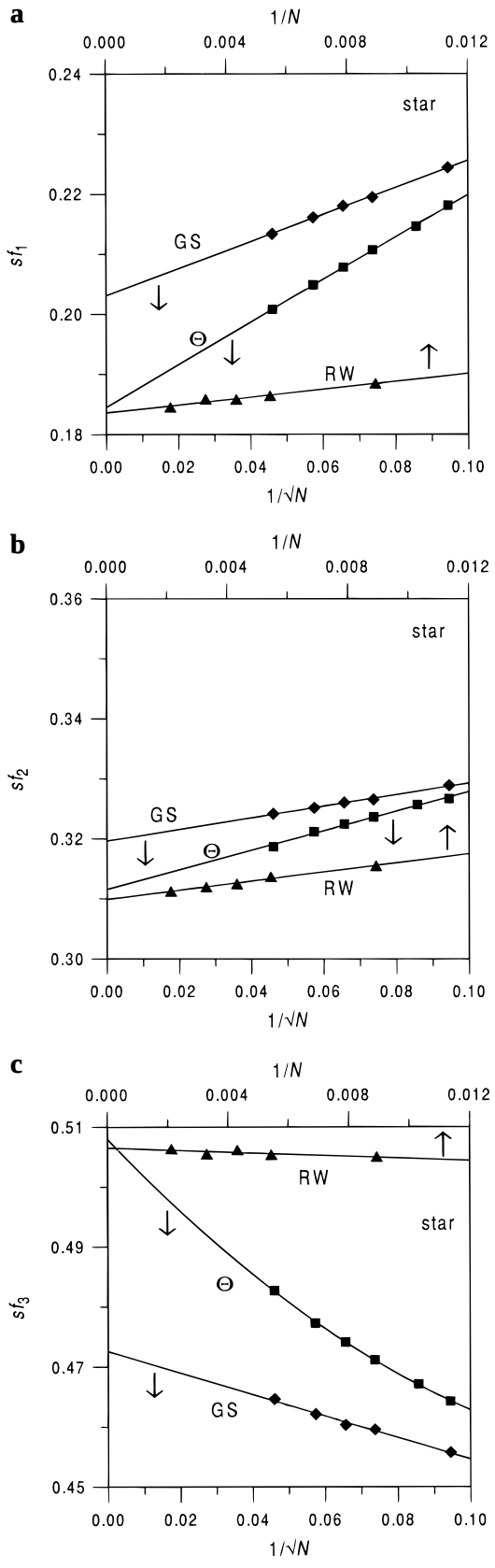

Figure 2. Shape factors sf_1, sf_2 and sf_3 (parts a, b, and c, respectively) of the stars in a good solvent (diamonds with GS label) and in the Θ state (squares with Θ label) plotted as a function of $N^{-1/2}$ (lower abscissa). The results for the random-walk polymers (triangles with RW label) are reported as a function of N^{-1} (upper abscissa) The best-fit curves are also shown.

moments approximate the random walk values, both for S^2 and for R^2. Incidentally, the second reduced moment

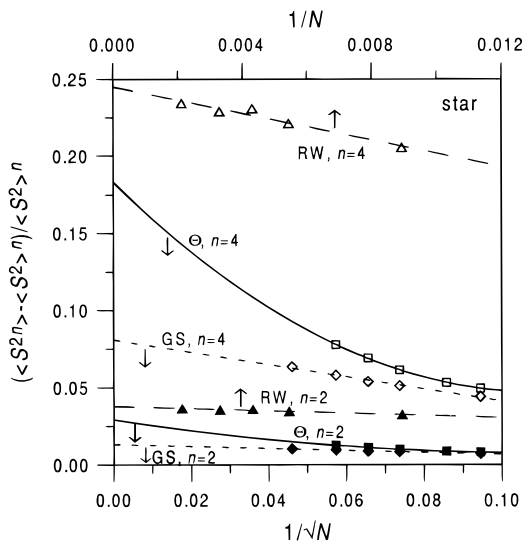

Figure 3. Reduced moments $\sigma_n^S = (\langle S^{2n}\rangle - \langle S^2\rangle^n)/\langle S^2\rangle^n$ with $n = 2$ (filled symbols) and $n = 4$ (open symbols) of the stars in a good solvent (diamonds with GS label) and in the Θ state (squares with Θ label) plotted vs $N^{-1/2}$ (lower abscissa). The results for the random-walk polymers (triangles with RW label) are also plotted vs N^{-1} (upper abscissa) The best-fit curves are also shown. The curves of the reduced moments with $n = 3$, not shown for clarity, are midway between those with $n = 2$ and $n = 4$.

of S^2, σ_2^S, confirms previous results of Monte Carlo simulations on a lattice[7,8] both for the asymptotic value and for the chain-length dependence, whereby σ_2^S increases with N. In the star the asymptotic reduced moments σ_n^R, $n = 2$, 3, 4, are again rather close to the random-walk values, whereas the reduced moments of S^2, σ_n^S, are appreciably smaller, the more so the larger n is (see Tables 1 and 2). In particular, the difference of σ_2^S from the random-walk value (about 0.01) is equal to that observed by Bruns and Carl[8] on linear and lightly branched chains ($f = 4$, 5, 6), whereas larger differences are found for σ_n^S, $n = 3$, 4. This result suggests that while the overall shape of a long star in the Θ state is very similar to the shape of a random-walk star, as discussed in the previous section, nonetheless the bead distribution within the molecule is greatly different. Moreover, from Figure 3 we see also that in the Θ state the reduced moments have a strong chain-length dependence: in particular, for small N they are almost indistinguishable from those in a good solvent. This behavior is again related to the large expansion in the core region which is present even in the Θ state and which encompasses most of the polymer for small N.

A greater insight about the bead distribution within the molecules is gained by the density profiles as a function of the distance r from the center of mass, reported in Figure 4. In order to meaningfully compare the various cases, we normalized the radial density profiles, $4\pi r^2\rho(r)$, through multiplication by $\langle S^2\rangle^{1/2}/N$. In this way, the curves plotted as a function of the normalized distance from the center of mass $r/\langle S^2\rangle^{1/2}$ have a unit area. Furthermore, we checked that, for each solvent regime and molecular architecture, the curves are independent of N, apart from very short chains, and so we report only the curves for the two largest N in each case. For a comparison, we also include the curves calculated from a Gaussian distribution around the center of mass with the appropriate second moment, i.e., $\langle S^2\rangle$. As expected, in all cases the

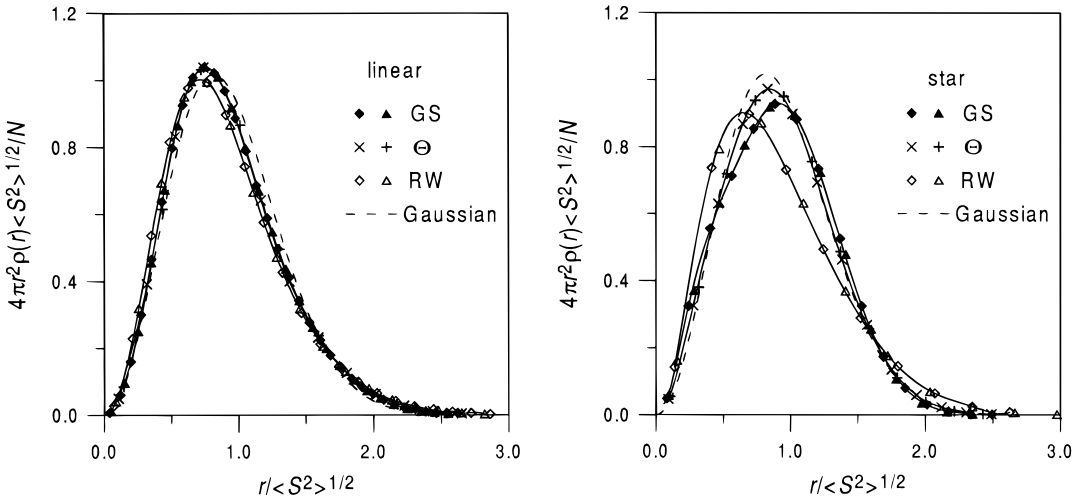

Figure 4. Normalized radial density profile $4\pi r^2\rho(r)\langle S^2\rangle^{1/2}/N$ plotted as a function of the normalized distance from the center of mass, $r/\langle S^2\rangle^{1/2}$, for linear and star polymers (left and right panels, respectively). Linear chains (left panel): diamonds, $N = 304$, and triangles, $N = 200$ (good solvent and random walk); ×, $N = 72$, and +, $N = 40$ (Θ state). Star chains (right panel): diamonds, $N = 304$, and triangles $N = 232$ (good solvent and random walk); ×, $N = 304$, and +, $N = 232$ (Θ state). The universal Gaussian curve is also reported for a comparison.

maximum of the distribution is located at distances from the center-of-mass close to $\langle S^2\rangle^{1/2}$, but some differences are significant. The normalized density profile of the linear chain in Figure 4, left panel, is basically the same in the good-solvent regime as in the Θ state, and is slighty shifted toward greater distances with respect to the random walk, due to the self-avoiding nature of the chain. In the star, however, the three cases are sharply distinct, and the curve maxima are increasingly shifted toward larger r's by going from the random-walk chain to the Θ state and then to the good-solvent conditions (see Figure 4, right panel). This is a further consequence of the large expansion in the core region, characterizing both Θ and good-solvent regimes: due to the inter- and the intraarm repulsions, the beads are much farther from the branch point than in the random walk, the effect being obviously more pronounced in a good solvent. On the other hand, the shift of the curve maxima involves a sharper decrease of the density profiles at larger r's, so that the two curves fall below the curve of the random walk when $r > 1.5\langle S^2\rangle^{1/2}$.

Concluding Remarks

In the present paper, we have reported the results of a study on the shape and size distribution of linear and 12-arm star polymers using an off-lattice Monte Carlo simulation.[2] In our previous work, we investigated in detail the local conformation of the star in a good solvent, showing that the star arms are largely uncorrelated in their directions, but at the same time they are also quite extended in the core region in order to best accommodate both the intra- and the interarm repulsions. Here we focus our attention on the behavior of finite chains under good-solvent conditions and in the Θ state for a comparison with lattice simulations, since in these cases contrasting results exist about the behavior of finite chains, unlike the asymptotic results that are independent of the lattice type. An important conclusion of our off-lattice simulations is that the local properties studied in paper I do have relevant consequences on the overall shape: for instance, finite star polymers are more spherical than stars with a very large molecular mass both under good-solvent conditions and in the Θ state because in both cases the local repulsions within each arm near the star core are dominant. Because of this factor, the same results are also obtained for any lattice type.[4,9] Conversely, in linear chains no such effect is present, and the dependence on the chain length is less pronounced. As a consequence, other factors may come into play, such as the local chain stiffness embodied in the characteristic ratio or, equivalently, in the chain persistence length. In turn, these parameters are related to the width of the repulsive part of the interaction potential, or they are implicitly embodied in the lattice type. Recent simulation results by Zifferer and Olaj on nonreversal random walks do indeed support this conclusion.[22]

Another important result of this work is that the molecular shape of the star in the Θ state closely resembles the shape of the corresponding random walk in the infinite chain limit, but this is not so for finite chains, and larger differences are present in the distribution of the beads within the molecule. In the case of relatively short chains, the shape of the star and its size distribution are much more similar to those in a good solvent than to those in a random walk because of the self-avoiding condition that still exists. Because of that, the large intraarm expansion is still present, and the chain behaves much as in a good solvent. For the same reason, the radial density profile around the center of mass is shifted at larger distances than in the random walk, with a significant bead depletion at short distances. The effect is clearly more pronounced in a good solvent. This also implies a faster density decrease at larger distances, such that the surface enclosing the star is much more sharply defined than in the linear chains, and its size distribution is much narrower.

Acknowledgment. We gratefully thank professor Giuseppe Allegra for useful discussions. This work was financially supported by the Italian Ministry for University and Scientific and Technological Research (MURST 40%) and by the Italian National Research Council (CNR, "Progetto Strategico Tecnologie Chimiche Innovative").

References and Notes

(1) Douglas, J. F.; Roovers, J.; Freed, K. F. *Macromolecules* **1990**, *23*, 4168.
(2) Forni, A.; Ganazzoli, F.; Vacatello, M. *Macromolecules* **1996**, *29*, 2994.

(3) Miyake, A.; Freed, K. F. *Macromolecules* **1983**, *16*, 1228; **1984**, *17*, 678.
(4) Batoulis, J.; Kremer, K. *Macromolecules* **1989**, *22*, 4277.
(5) See, e.g.: Allegra, G.; Ganazzoli, F. *Adv. Chem. Phys.* **1989**, *75*, 265.
(6) Allegra, G.; Colombo, E.; Ganazzoli, F. *Macromolecules* **1993**, *26*, 330.
(7) Mazur, J.; McCrackin, F. *Macromolecules* **1977**, *10*, 326.
(8) Bruns, W.; Carl, W. *Macromolecules* **1991**, *24*, 209.
(9) Zifferer, G. *Macromol. Theory Simul.* **1994**, *3*, 163.
(10) Lal, M. *Mol. Phys.* **1969**, *17*, 57. Stellman, S. D.; Gans, P. J. *Macromolecules* **1972**, *5*, 516. Zifferer, G. *Makromol. Chem.* **1990**, *191*, 2717.
(11) Metropolis, N.; Rosenbluth, A. W.; Rosenbluth, M. N.; Teller, A. H.; Teller, E. *J. Chem. Phys.* **1953**, *21*, 1087.
(12) Kajiwara, K.; Burchard, W. *Macromolecules* **1982**, *15*, 660.
(13) Rey, A.; Freire, J. J.; Bishop, M.; Clarke, J. H. R. *Macromolecules* **1992**, *25*, 1311.
(14) Zifferer, G. *Makromol. Chem., Theory Simul.* **1993**, *2*, 653.
(15) Kuhn, W. *Kolloid Z.* **1934**, *68*, 2.
(16) Šolc, K.; Stockmayer, W. H. *J. Chem. Phys.* **1971**, *54*, 2756.
(17) Šolc, K. *J. Chem. Phys.* **1971**, *55*, 335.
(18) Šolc, K. *Macromolecules* **1973**, *6*, 378.
(19) Rudnick, J.; Gaspari, G. *J. Phys. A* **1986**, *19*, L191.
(20) Wei, G.; Eichinger, B. E. *J. Chem. Phys.* **1990**, *93*, 1430.
(21) Fixman, M. *J. Chem. Phys.* **1962**, *36*, 306.
(22) Zifferer, G.; Olaj, O. F. *J. Chem. Phys.* **1994**, *100*, 636.
(23) Su, S.-J.; Denny, M. S.; Kovac, J. *Macromolecules* **1991**, *24*, 917.

MA970067F